



**HAL**  
open science

# Glass, crystallization and phase separation an insight into glass enriched in MoO<sub>3</sub>

S. Schuller, S. Gossé, J. Rogez

► **To cite this version:**

S. Schuller, S. Gossé, J. Rogez. Glass, crystallization and phase separation an insight into glass enriched in MoO<sub>3</sub>. Joint ICTP-IAEA Workshop on Fundamentals of Vitrification and Vitreous Materials for Nuclear Waste Immobilization (smr 3159), Nov 2017, Trieste, Italy. cea-02400187

**HAL Id: cea-02400187**

**<https://cea.hal.science/cea-02400187>**

Submitted on 9 Dec 2019

**HAL** is a multi-disciplinary open access archive for the deposit and dissemination of scientific research documents, whether they are published or not. The documents may come from teaching and research institutions in France or abroad, or from public or private research centers.

L'archive ouverte pluridisciplinaire **HAL**, est destinée au dépôt et à la diffusion de documents scientifiques de niveau recherche, publiés ou non, émanant des établissements d'enseignement et de recherche français ou étrangers, des laboratoires publics ou privés.

# GLASS, CRYSTALLIZATION AND PHASE SEPARATION: AN INSIGHT INTO GLASS ENRICHED IN MoO<sub>3</sub>

S. SCHULLER<sup>1</sup>, S. GOSSÉ<sup>2</sup>, J. ROGEZ<sup>3</sup>

<sup>1</sup>CEA, DEN, DE2D, SEVT F-30207 Bagnols-sur-Cèze, France

<sup>2</sup>DEN-Service de la Corrosion et du Comportement des Matériaux dans leur Environnement (SCCME), CEA, Université Paris-Saclay, F-91191, Gif-sur-Yvette, France

<sup>3</sup>IM2NP Aix Marseille Univ, Univ Toulon, CNRS, Faculté des Sciences de St Jérôme, Service 251, avenue Normandie-Niémen, 13397 Marseille, France

## Abstract

Highly focused research programs are currently underway in CEA Marcoule to develop and optimize vitrification processes for the production of waste containment glasses. The main issues facing us today are to accommodate new types of waste and higher waste loading, while enhancing the glass quality and increasing the production capacity and robustness of the plants. This requires extensive knowledge of the physical and chemical properties of glassy materials. Academic research on glass melting is conducted to understand the phenomenology behind the formation of the glass and its evolution after cooling from atomic to macroscopic scale. Understanding the physical and chemical properties of glass in the liquid and solid state is a major challenge to allow increased waste loading and the development of new glass formulations. In this paper we illustrate the contribution of this research considering the phases separation and crystallisation process in glass enriched in MoO<sub>3</sub>. We show in particular how the thermodynamic and structural aspects can elucidate the mechanism of incorporating molybdenum oxide in alkali borosilicate glass.

## 1. INTRODUCTION

The composition of nuclear glasses are very complex mixtures of elements coming from the nuclear wastes such as fission products, actinides and corrosion products, with others coming from the glass precursors (Figure 1). Wastes are integrated in the vitreous network by reactions occurring in vitrification furnaces set to operate at temperatures generally between 1000°C and 1200°C. The state of the precursors and waste microstructures evolve with time and temperature until a high-temperature homogeneous liquid is formed. The final glass package is then obtained by cooling and solidifying the liquid into a metallic container.

During the different steps of the process, the fission products and actinides can be integrated into the glass structure up to an incorporation limit. Beyond this limit, volatilization or heterogeneity formation may occur in the case of certain volatile RN (<sup>129</sup>I, <sup>36</sup>Cl, <sup>137</sup>Cs, <sup>99</sup>Tc, <sup>106</sup>Ru) or for those with a low incorporation capacity (high oxidation state anions and cations) [1]. These fission products incorporations also depend on the glass manufacturing conditions such as temperature, mixing conditions, reaction time.

The waste loading must be limited in order to obtain a homogeneous glass at the microscopic scale (R7T7 glass is an example of industrial glass currently produced in La Hague processing plant inside hot crucible melters) [2],[3]. In order to contain larger quantities of packaged wastes, it is also possible to go beyond the incorporation limits by using macroscopically homogeneous vitro-crystalline or vitro-ceramic matrices (UMo glass is another example of industrial glass also produced in cold crucible melter) [4].



## 2. THERMODYNAMIC DESCRIPTION OF PHASE SEPARATION

### 2.1. Ideal solution, solubility

Two entities A and B are miscible in any proportions at a given temperature ( $T$ ) when they mix completely with each other. From an energy standpoint, the formation of such a mixture is characterized by the free energy of mixing ( $\Delta_{mix}G$ ) which corresponds to the difference between the total free energy of the solution after mixing ( $G_m$ ) and before mixing ( $G_{tot}$ ), defined by the following equations:

$$\Delta_{mix}G = G_m - G_{tot} = n_A(\mu_A - \overline{G}_A^0) + n_B(\mu_B - \overline{G}_B^0)$$

where  $\Delta_{mix}G$  is the Gibbs free energy of mixing,  $n_A$  and  $n_B$  the number of moles of components A and B,  $\mu_A$  and  $\mu_B$  the partial molar free energies of entities A and B.

$$\Delta_{mix}G = \Delta_{mix}H - T\Delta_{mix}S$$

where  $\Delta_{mix}H$  is the enthalpy of mixing and  $\Delta_{mix}S$  is the entropy of mixing.

Mixing results in an “ideal” solution if the volume and enthalpy variations are zero ( $\Delta_{mix}V^{id}=0$ ,  $\Delta_{mix}H^{id}=0$ ). The variations of the ideal entropy ( $\Delta_{mix}S^{id}$ ) and the Gibbs free energy ( $\Delta_{mix}G$ ) of mixing during the formation of the solution thus depend only on the concentrations of its constituents:

$$\Delta_{mix}S^{id} = R[X_A \ln X_A + X_B \ln X_B]$$

$X_A$  and  $X_B$  are the mole fractions of substances A and B, respectively. The free energy between compounds A and B varies monotonically with the composition as shown in Figure 3.

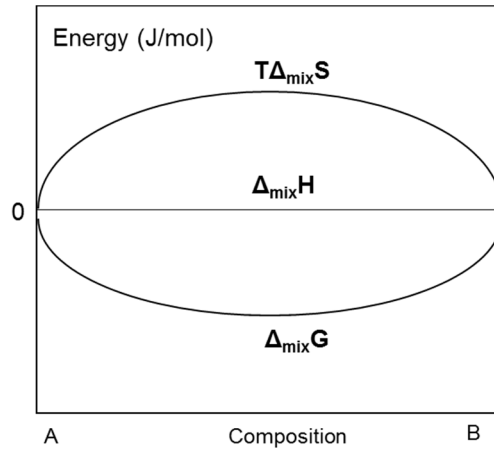


FIG 3: Variation of Gibbs free energy, and entropy of mixing during ideal mixing of two pure entities A and B.

The solubility is defined as the maximum concentration of an entity (solute A) that can be contained in a phase (solvent B) under specified conditions of temperature, pressure, and chemical composition of other entities in the case of complex mixtures.

## 2.2. Regular solution and immiscibility

The thermodynamically description of phase separation in a glass is closely the same to that in solid of same structure or liquid solutions. From the energy standpoint, the appearance of two immiscible liquids in a binary system is associated with a positive enthalpy of mixing (Figure 4a).

At a given temperature the solution will be stable if the Gibbs free energy of mixing ( $\Delta_{mix}G$ ) remains negative over the full composition range (Figure 4b). As the entropic contribution largely overcome in term of absolute value the enthalpic positive term, the solution remains stable (Figure 4b).

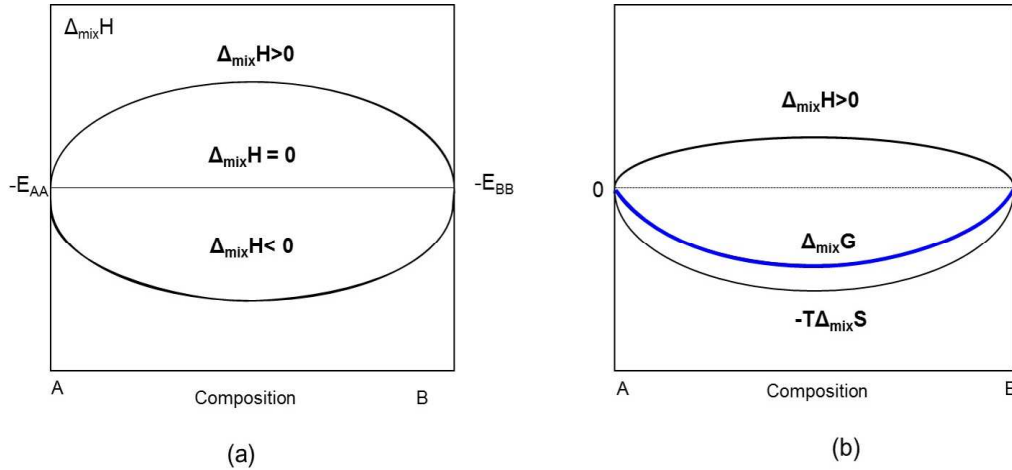


FIG 4: (a) Variation of  $\Delta_{mix}H$  versus composition. The deviation from ideality ( $\Delta_{mix}H = 0$ ) is negative or positive. (b) Variation of Gibbs free energy  $\Delta_{mix}G$ , without any phase separation, contributions of a positive deviation of enthalpy of mixing ( $\Delta_{mix}H$ ), counterbalanced by an higher entropy contribution ( $-T\Delta_{mix}S$ )

A higher mixing enthalpy ( $\Delta_{mix}H \gg 0$ ) results in instability of the solution at low temperatures, because of the relative decrease, in absolute value, of the magnitude of the entropic term  $-T\Delta_{mix}S$ . At high temperatures the entropic term predominates and the Gibbs free energy has a single minimum (Figure 5-a). At lower temperatures ( $T_1$ ) the entropic term diminishes and the enthalpic term becomes predominant. This effect results in immiscibility when  $X_{A1} > X_M > X_{B1}$  at  $T_1$  for example. These mechanisms are revealed by the existence of two liquids of different compositions separated by a binode or solvus coexistence curve that defines the extent of the miscibility gap as a function of the temperature (Figure 5-b). Above a critical temperature ( $T_C$ ), also known as the consolute temperature, the stable phase is a unique liquid ( $L$ ) and the Gibbs free energy of mixing  $\Delta_{mix}G(T)$  exhibits only a single minimum. Lowering the temperature below  $T_C$  results in a change in the Gibbs free energy which in this case exhibits two minima responsible for the separation into two phases.

Most often, solutions deviates from ideality and may behave as “regular” or “real” solutions. In this cases, the thermodynamics functions of the solution differ from the ones of a weighted mixture of the references having the same global composition as the solution.

The deviation from ideality and its effect on the process of phase separation can be indicated by  $\Delta_{mix}H$  functions taking into account the characteristic parameters of the interaction force,  $\Lambda$ , between entities A and B. The function enthalpy can often be characterized by a strictly regular solution.

$$\Delta_{mix}H = \Lambda X_A X_B$$

$$\Lambda = -ZN_A \left( E_{AB} - \frac{1}{2}(E_{AA} + E_{BB}) \right)$$

where  $Z$  is the coordination number of the entities in the solution, assumed to be identical for A and B entities,  $N_A$  is Avogadro's number,  $E_{AB}$  is the energy of hetero-interactions between entities A and B, and  $E_{AA}$  and  $E_{BB}$  the energies of homo-interactions between A or B entities.

Together with the variation of enthalpy and entropy the variation of the Gibbs free energy function,  $\Delta_{mix}G$ , describes the process of the phase separation in a strictly regular solution which corresponds to:

$$\Delta_{mix}G = \Lambda X_A X_B - RT[X_A \ln X_A + X_B \ln X_B]$$

In the sense of the Calphad method, the Gibbs free energy function is written as a sum of the Gibbs free energies of the references and of ideal and excess Gibbs free energies:

$$\Delta_{mix}G = \Delta G^0 + \Delta G^{Id} + \Delta G^E$$

$$\Delta_{mix}G = X_A^0 G_A + X_B^0 G_B - RT[X_A \ln X_A + X_B \ln X_B] + \Lambda X_A X_B$$

The interaction parameter  $\Lambda$  is one of the most important parameter in the phase separation phenomena because it determines positive or negative sign of the excess Gibbs energy of the regular solution. In the case of repulsive interaction, the parameter is positive and the solution tends to separate into two distinct composition sets. This parameter can be correlated to the structure of the glass.

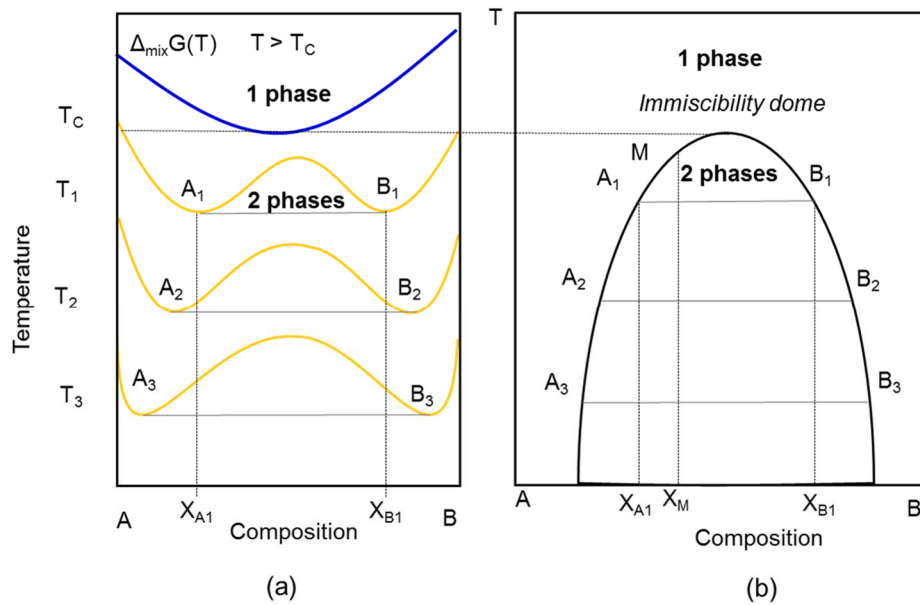


FIG 5: (a) Gibbs free energy ( $\Delta_{mix}G(T)$ ) variation as a function of Temperature. (b) Schematic representation of a coexistence curve on a binary temperature/composition diagram

### 3. INFLUENCE OF THE STRUCTURE ON THE PHASE SEPARATION TENDENCY

As it shown by Kracek [5] in silica oxide systems, the tendency to phase separation increased with the cation field strength of alkali and alkaline earth. The importance of the lower plateau with two liquids, indicating the greatest extent of the miscibility gap (Figure 6), can indeed be correlated to the field strength of the cations,  $Z/r$  ( $Z$  = oxidation number,  $r$  = ionic radius of the cation).

Mazurin [6] has shown similar behavior in the case of borosilicate glasses (Figure 7) for ternary systems ( $R_2O-B_2O_3-SiO_2$ ),  $R$  = Li, Na, K, Rb, Cs.

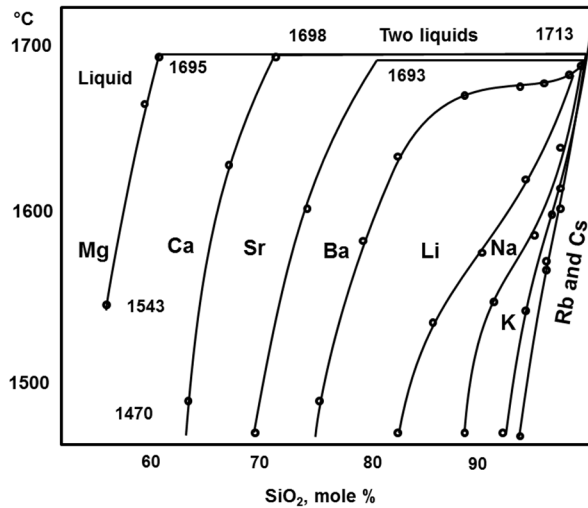


FIG 6: Equilibrium diagram of binary silica-alkali oxide and silica-alkaline-earth oxide systems for cations such as  $\text{Na}^+$ ,  $\text{Li}^+$  and  $\text{Ba}^{2+}$ , the S-shaped liquidus curve includes a portion with an inflection characteristic of nearby underlying metastable phase separation. For  $\text{Mg}^{2+}$ ,  $\text{Ca}^{2+}$  and  $\text{Sr}^{2+}$  cations with a higher field strength, stable phase separation is observed at high temperatures (from Kracek, 1930 [5]).

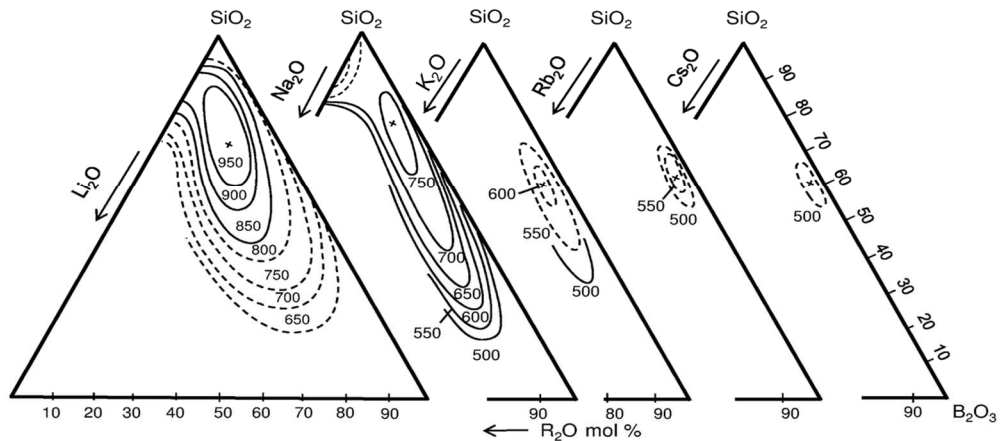


FIG 7: Miscibility gaps in isothermal cross sections of ternary systems ( $\text{R}_2\text{O}-\text{B}_2\text{O}_3-\text{SiO}_2$ ),  $\text{R} = \text{Li}, \text{Na}, \text{K}, \text{Rb}, \text{Cs}$  (from Mazurin et al., 1984,[6]).

The ternary  $\text{SiO}_2-\text{Na}_2\text{O}-\text{MoO}_3$  system presents a large immiscibility domain experimentally highlighted by Stemprok [7] at 1473 K. These experimental results also reveal that the demixing phenomenon comes from repulsive interactions in the  $\text{MoO}_3-\text{SiO}_2$  pseudo-binary diagram (i.e. there are no liquid miscibility gaps in both  $\text{Na}_2\text{O}-\text{MoO}_3$  and  $\text{Na}_2\text{O}-\text{SiO}_2$  systems).

Using the Calphad method, Gossé et al. [8] performed a thermodynamic assessment to highlight the phase separation in liquid silicates due to molybdenum oxides. The calculations are in good agreement with the experimental points from Stemprok (Figure 8-a). For this reason, the binary  $\text{MoO}_3-\text{SiO}_2$  liquid is modeled by a regular repulsive interaction parameter (+70 kJ/mol/at) between the  $\text{MoO}_3$  and the  $\text{SiO}_2$  liquid species [8]. This leads to two minima in the Gibbs free energy, responsible for the separation into two composition sets represented in the 1273-2073 K temperature range (Figure 8-b).

It is also seen in Figure 8-a that, in the ternary region containing less than 60 molar % of  $\text{Na}_2\text{O}$ , the miscibility gap separates in two liquids, one silica rich liquid depleted in  $\text{MoO}_3$  and the other enriched in  $\text{MoO}_3$  very close to the  $\text{Na}_2\text{MoO}_4$  composition. Due to this liquid composition,  $\text{Na}_2\text{MoO}_4$  crystals can precipitate easily on further cooling as indicated by the orientation of the tielines in the liquid miscibility

gap. From this thermodynamic approach, a link between the extent of the miscibility gap and the structure of glass can be established in the ternary  $\text{SiO}_2\text{-Na}_2\text{O-MoO}_3$  system.

Molybdenum is mainly under at +VI oxidation state in silicate and borosilicate glasses prepared under oxidizing conditions; molybdenum forms  $\text{MoO}_4^{2-}$  tetrahedral units distributed in depolymerized areas of glass with charge-compensating cations (alkalis and alkaline-earths) [9]-[13].

According to Mo K-edge EXAFS results, the average Mo–O distance  $d(\text{Mo-O})$  in silicate and borosilicate glasses is  $\approx 1.8 \text{ \AA}$  and the calculated cation field strength  $F$  of  $\text{Mo}^{6+}$  calculated by  $6/d(\text{Mo-O})^2$ , corresponds to  $\approx 1.85 \text{ \AA}^{-2}$  [14]. Furthermore according to Pauling's stability rules [15], it has been shown that the  $\text{MoO}_4^{2-}$  specy cannot be directly connected to the silicate network [16].

Indeed, the existence of Mo–O–Si linkages between  $\text{MoO}_4$  and  $\text{SiO}_4$  units would imply that the sum of the bond valences  $S_{\text{Mo-O}} + S_{\text{Si-O}} \approx 2.5\text{--}2.6$  valence units are indeed greater than 2. In such configuration the oxygen atom would be strongly overbonded and the linkage between molybdenum and silicon oxides is not possible. Consequently,  $\text{Mo}^{6+}$  cation apply a strong ordering effect on the surrounding oxygen anions and the only cations that can achieve charge compensation around  $\text{MoO}_4^{2-}$  entities should be alkali or alkaline-earth cations.

Then,  $\text{MoO}_4^{2-}$  entities may easily separate from the silicate or borosilicate glassy network in a depolymerized area promoting a repolymerization of the remaining silicate or borosilicate network [14],[17]. Moreover, this mechanism occurs probably at an atomic scale by the clustering of several isolated molybdate units on one side and silica on the other. Nicouleau [18] has shown that in sodium borosilicate glasses enriched in  $\text{MoO}_3$ , a low  $\text{MoO}_3$  concentration (0.5% molar) leads to a polymerization of the silicate network (characterised by  $^{29}\text{Si}$  MAS NMR) while a higher concentration (up to 2% molar) decreases the number of tetrahedral boron (characterised by  $^{11}\text{B}$  MAS NMR).

Furthermore, it is demonstrated that the non-bridging oxygens, which mobilizes two atoms of sodium, is correlated to the quantity of separated phases containing  $\text{Na}_2\text{MoO}_4$  crystals after cooling due to the repolymerization of the silicate network.

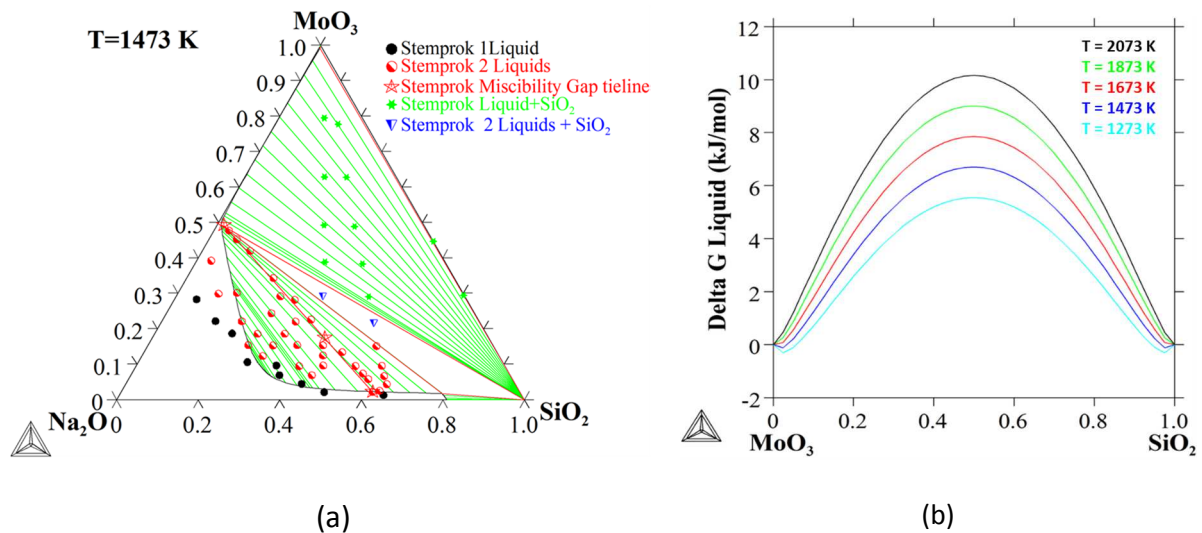


FIG 8: (a) Immiscibility gaps in isothermal cross sections 1473 K of ternary systems  $\text{SiO}_2\text{-Na}_2\text{O-MoO}_3$  modeling by CALPHAD method [8] compared to experimental data from Stemprok [7] (b)  $\Delta G_{\text{liq}}$  evolution with temperature in the binary  $\text{MoO}_3\text{-SiO}_2$  system

#### 4. MECHANISM OF PHASE SEPARATION AND CRYSTALLISATION IN BOROSILICATE ENRICHED IN MOLYBDENUM OXIDE

When the molybdenum oxide content is higher than a solubility limit which is around 1-1.5 % molar in simplified borosilicate glasses at room temperature [19], non-homogenous glasses are formed through

a sequence of phase separation and crystallization on cooling. The phenomenon starts by a liquid–liquid phase separation at high temperature, then the liquid enriched in molybdenum oxide partially crystallizes on cooling under the form of alkali and alkaline-earth molybdates [20]-[22]

Depending on the glass composition, crystalline alkali or alkali earth molybdates such as  $\text{Li}_2\text{MoO}_4$  [23],  $\text{Na}_2\text{MoO}_4$ ,  $\text{CaMoO}_4$  [24]-[28],  $\text{MgMoO}_4$  [29], or more complex poly-molybdates containing two different alkali elements such as  $\text{CsNaMoO}_4$ ,  $\text{Cs}_3\text{Na}(\text{MoO}_4)_2$  [30],[31]  $\text{CsLiMoO}_4$  [32]  $\text{Na}_3\text{Li}(\text{MoO}_4)_2$  [33] are detected after cooling in a wide range of silicate and borosilicate non-radioactive glass compositions.

This mechanism of liquid-liquid phase separation has been observed by high-temperature environmental SEM in sodium borosilicate glass enriched in  $\text{MoO}_3$ . The influence of  $\text{MoO}_3$  concentration is illustrated in Figure 9. HT-ESEM analyses performed at  $750^\circ\text{C}$  (below the phase separation temperature) revealed qualitatively that the quantity of the liquid separated phase enriched in  $\text{MoO}_3$  and  $\text{Na}_2\text{O}$  (and also depleted in  $\text{SiO}_2$ ) increases with the  $\text{MoO}_3$  concentration as the demixion is greater. On the thermodynamic point of view, this result is consistent with the lever rule.

It has been shown in many glass-forming systems that the mechanism of phase separation differs according to the initial glass composition. A description of the Gibbs free energy variation during the phase separation process can distinguish two domains where phase separation occurs by nucleation and growth or by spinodal decomposition [34],[35]. The nature, the composition, and the morphology of the separated phases are different inside or outside the spinode curve defining the boundary between these two modes of separation. Separated phases formed by a nucleation and growth process are spherical and disconnected. They are characterized by a sharp interface and a composition that does not change with time. Conversely, when the mechanism occurs by spinodal decomposition the phases are interconnected and their composition and morphology are modified over time.

In the case of phase separation promoted by molybdenum oxide (Figure 9, 10), separated phases are already spherical, dispersed randomly, disconnected and the morphology remains identical with a variation of  $\text{MoO}_3$  concentration (up to 10 % molar  $\text{MoO}_3$ ).

These microstructural observations reveal that the process occurs near the binodal curve in the zone of nucleation and growth.

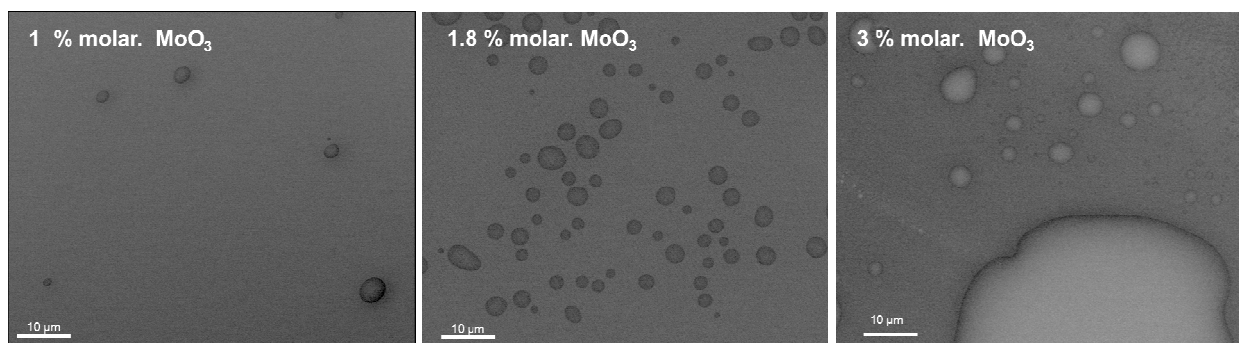


**FIG 9:** High-temperature environmental SEM images of phase separation obtained by nucleation and growth in sodium borosilicate glass  $\text{SiO}_2\text{-Na}_2\text{O-B}_2\text{O}_3\text{-MoO}_3$  containing 1, 1,8 and 3 % molar  $\text{MoO}_3$  during a heat treatment at  $750^\circ\text{C}$ .

After cooling, the glass remaining is partially crystallized (Figure 10). SEM analysis of a glass sample containing 3% molar  $\text{MoO}_3$  ( $61\text{SiO}_2\text{-}19\text{Na}_2\text{O}\text{-}16\text{B}_2\text{O}_3\text{-}3\text{MoO}_3$ ) shows the presence of separated phases with diameters –i-less than  $1\ \mu\text{m}$  and –ii-greater than  $30\ \mu\text{m}$  which contain visible crystalline phases inside the separated phases corresponding to  $\text{Na}_2\text{MoO}_4$  and  $\text{Na}_2\text{Mo}_2\text{O}_7$  (see details of the structure in [18])

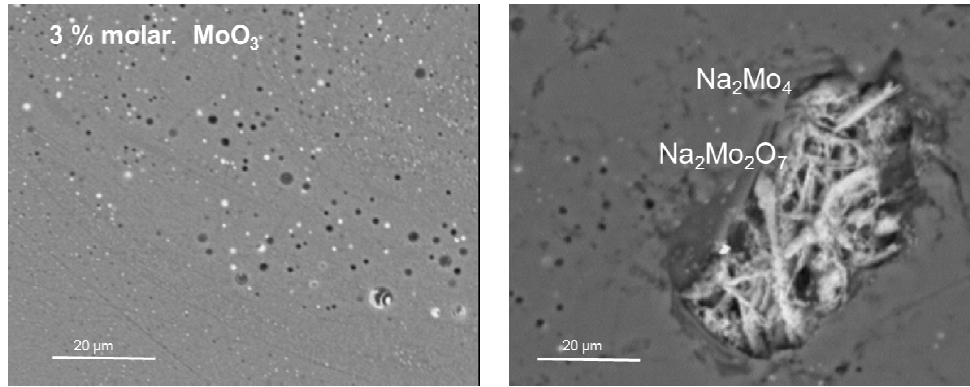


FIG 10: SEM Images of crystalline separated phase obtained after glass synthesis ( $61\text{SiO}_2\text{-}19\text{Na}_2\text{O-}17\text{B}_2\text{O}_3\text{-}3\text{MoO}_3$ ) containing 3% molar.  $\text{MoO}_3$  at  $1300^\circ\text{C}$  and cooling at  $10^3^\circ\text{C/min}$

Based on these results and on previous studies [20],[21],[30], these processes of phase separation and crystallization can be represented by the free energy-composition simplified diagram for  $\text{SiO}_2\text{-MoO}_3$  for a temperature below phase separation temperature (Figure 11-a).

At  $T < T_c$ , an initial glass composition (M) can minimize its Gibbs energy by an equilibrium between the phases A and B along the common tangent AB. Liquid-liquid phase separation leads to a liquid phase A enriched in  $\text{SiO}_2$  depleted in  $\text{MoO}_3$ , and a liquid phase B enriched in  $\text{MoO}_3$  containing a residual amount of  $\text{SiO}_2$ . Below the liquidus temperature, the phase B crystallizes. A second equilibrium is established along tangent CD. In accordance with the mass balance, liquid phase B evolves toward its stable state with the formation of phase C and a new phase D enriched in  $\text{SiO}_2$ . The vitreous phase E is never formed at the experimental time scale due to the metastability of the glass D.

The mechanism is characterized in alkali, alkaline earth borosilicate glasses by the formation of a mixture of crystalline phases ( $\text{Na}_2\text{MoO}_4$ ,  $\text{CsNaMoO}_4$ ,  $\text{Li}_2\text{MoO}_4$ ,  $\text{Na}_2\text{MoO}_4$ ,  $\text{CaMoO}_4$ ,  $\text{MgMoO}_4$ ,  $\text{CsNaMoO}_4$ ,  $\text{Cs}_3\text{Na}(\text{MoO}_4)$ ,  $\text{CsLiMoO}_4$ ,  $\text{Na}_3\text{Li}(\text{MoO}_4)_2, \dots$ ), phase C, and a residual glass enriched in  $\text{SiO}_2$ ,  $\text{B}_2\text{O}_3$  (phase D) within the separated phases (phase B).

Figure 11-b gives an illustration in a sodium, cesium borosilicate glass ( $62\text{SiO}_2\text{-}16.5\text{B}_2\text{O}_3\text{-}16\text{Na}_2\text{O-}3\text{Cs}_2\text{O-}2.5\text{MoO}_3$ ) containing 2.5 % molar  $\text{MoO}_3$ . After cooling ( $10^3^\circ\text{C/min}$ ), spherical separated phases (phase B) containing crystalline phases ( $\text{Na}_2\text{MoO}_4$  and complex sodium cesium molybdates - phase C) and a residual vitreous phase (glass beads - phase D) enriched in  $\text{SiO}_2$  and  $\text{B}_2\text{O}_3$  are characterized by SEM.

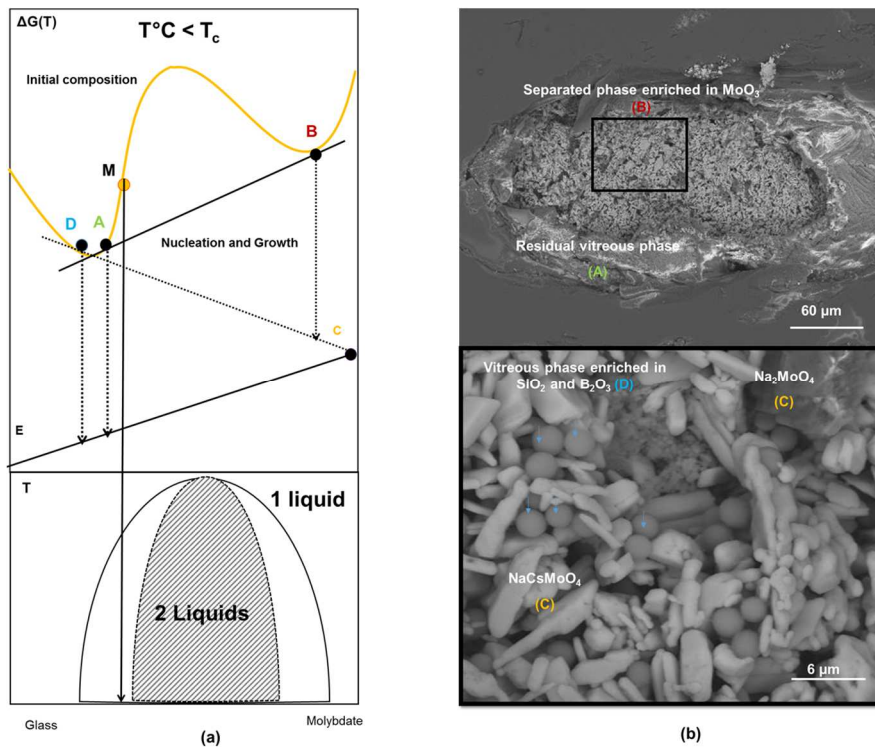


FIG 11: (a) Schematic representation of Gibbs free energy/composition diagram of pseudo binary  $\text{SiO}_2\text{-MoO}_3$  (b) SEM images of crystalline separated phases obtained after cooling in a sodium, cesium borosilicate glass containing 2,5% molar  $\text{MoO}_3$ .

## 5. CONCLUSIONS

Experimental and theoretical approaches, based on thermodynamic and structural aspects are relevant to better predict the mechanism of phase separation and crystallization of borosilicate glasses enriched in  $\text{MoO}_3$ . Explanations related to the low solubility of  $\text{MoO}_3$  and the two-step processes of phase separation and crystallization have been given. This approach highlighted the complexity to stabilize  $\text{MoO}_3$  in borosilicate glass above to 1-1.5 % molar  $\text{MoO}_3$  and to found the best compromise to increase the waste loading in containment glasses. The stimulating challenges in the coming years for the international community is to develop new glasses or glass-ceramics waste formed up to 20 % waste loading. In parallel, current researches focused on the incorporation of  $\text{MoO}_3$  and rare earth oxide are carried out in a wide range of compositions for the immobilization of fission-product waste streams [27][28],[36][41].

## 6. ACKNOWLEDGEMENTS

This work was funded by the Commissariat à L'Énergie Atomique et aux Énergies Alternatives. Financial support by ORANO is also gratefully acknowledged. The authors thank the CNRS research group (GDR) "TherMatHT for collaborative work, J. Ravoux and R. Podor for performing ESEM analyses at the ICSM (Marcoule, France) and IAEA for organizing "Joint ICTP-IAEA Workshop on Fundamentals of Vitrification and Vitreous Materials for Nuclear Waste Immobilization" in Trieste, November 2017. The authors particularly grateful to P. Benigni for the careful rereading of this paper.

## REFERENCES

- [1] GIN S., JOLLIVET P., TRIBET M., PEUGET S., SCHULLER S., “Radionuclides containment in nuclear glasses: An overview” *Radiochimica Acta* **105** (11) pp. 927–959 (2017) DOI 10.1515/ract-2016-2658
- [2] PETITJEAN V., FILLET C., BOEN R., VEYER C., FLAMENT T., “Development of vitrification process and glass formulation for nuclear waste conditioning”; WM’02 Conference, February 24–28, Tucson, AZ (2002)
- [3] VERNAZ E., BRUEZIÈRE J., “History of Nuclear Waste Glass in France”; *Procedia Materials Science* 7 SumGLASS 2013, 2nd International Summer School on Nuclear Glass Wasteform: Structure, Properties and LongTerm Behavior, pp 3-9 (2014)
- [4] PINET O., HOLLEBECQUE J.F., ANGELI F., GRUBER P., “Vitrification of Molybdenum-Rich High-Level Solutions by the Cold Crucible Melter Process”; WM2011 Conference, February 28–March 3, Phoenix, AZ (2011)
- [5] KRACEK F.C., “Cristobalite liquidus in alkali oxide-silica systems and heat of fusion of cristobalite”; *J. Am. Chem. Soc.*, **52**, pp 1436-1442 (1930).
- [6] MAZURIN O.V., PORAI-KOSHITS E.A., ANDREEV N.S., “Phase separation in glass”; North-Holland, Amsterdam & New-York. (1984)
- [7] STEMPROK M., *International Geology Review*. **17**, pp. 1306-1316 (1975)
- [8] GOSSE S., GUENEAU C., BORDIER S., SCHULLER S., LAPLACE A, ROGEZ J., “A thermodynamic approach to predict the metallic and oxide phases precipitation in nuclear waste glass melts ” *Procedia Material Science* ; 7, pp 79-86 (2014)
- [9] CALAS G., LE GRAND M., GALOISY L., GHALEB D., “Structural role of molybdenum in nuclear glasses: an EXAFS study”; *J. Nucl. Mater.* **322**, pp. 15-20 (2003)
- [10] SHORT R.J. , HAND R.J., HYATT N.C., “Molybdenum in nuclear waste glasses - incorporation and redox state”; *Mater. Res. Soc. Symp. Proc.* **757**, pp. 141-146 (2003)
- [11] SHORT R.J. , HAND R.J. , HYATT N.C. , MÖBUS G., “Environment and oxidation state of molybdenum in simulated high level nuclear waste glass compositions” *J. Nucl. Mater.* **340**, pp. 179-186 (2005)
- [12] HORNEBER, B. CAMARA, W. LUTZE “Investigation on the oxidation state and the behaviour of molybdenum in silicate glass” *Mater. Res. Soc. Symp. Proc.***11**, pp. 279-288 (1982)
- [13] FARGES F., SIEWERT R., BROWN G.E., GUESDON A., MORIN G., “Structural environments around molybdenum in silicate glasses and melts. I. Influence of composition and oxygen fugacity on the local structure of molybdenum” *Can. Mineral* **44**, pp. 731-753 (2006)
- [14] CAURANT D., MAJÉRUS O., FADEL E., QUINTAS A., GERVAIS C., CHARPENTIER T., NEUVILLE D., “Structural investigations E. of borosilicate glasses containing MoO<sub>3</sub> by MAS NMR and Raman spectroscopies”; *J. Nucl. Mater.* **396**, pp. 94-101(2010)
- [15] PAULING L., “The principles determining the structure of complex ionic crystals”; *J. A. Chem Soc.* **51**, Issue 4, pp. 1010-1026 (1929)
- [16] GALOISY L., CORMIER L., ROSSANO S., RAMOS A., CALAS G., GASKELL P., LE GRAND M., *Mineral. Mag.*, **64**, pp. 207-222 (2000)
- [17] MARTINEAU C., MICHAELIS V.K., SCHULLER S., KROEKER S., “Liquid–liquid phase separation in model nuclear waste glasses: a solid-state double-resonance NMR study” *Chem. Mater.* **22**, pp. 4896-4903 (2010)
- [18] NICOLEAU E., SCHULLER S., ANGELI F., CHARPENTIER T., JOLLIVET P., LE GAC A., FOURNIER M., MESBAH A., VASCONCELOS F., “Phase separation and crystallization effects on the structure and durability of molybdenum borosilicate glass”; *Journal of Non-Crystalline Solids*, **427**, pp. 120-133 (2015)
- [19] BENIGNI P., ROGEZ J., SCHULLER S., “Experimental Determination of Thermodynamical Quantities in Oxide Mixtures and Glasses”; *Procedia Materials Science*, **7**, pp. 138-147 (2014)

- [20] SCHULLER S., PINET O., PENELON B., “Liquid–liquid phase separation process in borosilicate liquids enriched in molybdenum and phosphorus oxides”; *J. Am. Ceram. Soc.* **94**, pp. 447-454 (2011)
- [21] MAGNIN M., SCHULLER S., CAURANT D., MAJERUS O., DE LIGNY D., ADVOCAT T., “Phase Separation and Crystallization in Soda-Lime Borosilicate Glass Enriched in MoO<sub>3</sub>”; in *Proceedings of Atalante 2008 Nuclear Fuel Cycles for Sustainable Future*, Atalante, Montpellier, France, (2008)
- [22] MAGNIN M., SCHULLER S., CAURANT D., MAJERUS O., DE LIGNY D., “Study of molybdenum incorporation in nuclear waste glass: effect of compositional variations in borosilicate glasses rich in MoO<sub>3</sub>”; *Proceedings of Global 2009 – paper 9288. International conference Global 2009*, Paris (2009)
- [23] KROEKER S., FARNAN I., SCHULLER S., ADVOCAT T., “<sup>95</sup>Mo NMR Study of Crystallization in Model Nuclear Waste Glasses”; pp. 153–9 in *Scientific Basis for Nuclear Waste Management XXXIV*, Vol. 1124, Edited by R. B. Rebak, N. C. Hyatt, and D. A. Pickett. Materials Research Society, Warrendale, PA, (2009)
- [24] MAGNIN M., SCHULLER S., CAURANT D., MAJÉRUS O., De LIGNY D., MERCIER C., “Effect of compositional changes on the structure and crystallization tendency of a borosilicate glass containing MoO<sub>3</sub>”; *Ceram. Trans.* **207**, pp. 59-67 (2009)
- [25] MAGNIN M., SCHULLER S., MERCIER C., TREBOSC J., CAURANT D., MAJÉRUS O., ANGELI F., CHARPENTIER T., “Modification of molybdenum structural environment in borosilicate glasses with increasing content of boron and calcium oxide by <sup>95</sup>Mo MAS NMR” *J. Am. Ceram. Soc.* **94**, pp. 4274-4282 (2011)
- [26] CAURANT D., MAJÉRUS O., FADEL E., LENOIR M., GERVAIS C., PINET O., “Effect of molybdenum on the structure and on the crystallization of SiO<sub>2</sub>–Na<sub>2</sub>O–CaO–B<sub>2</sub>O<sub>3</sub> Glasses” *J. Am. Ceram. Soc.* **90**, pp. 774-783 (2007)
- [27] CRUM J.V., TURO L., RILEY B., TANG M., KOSSOY A., “Multi-Phase Glass-Ceramics as a Waste Form for Combined Fission Products: Alkalis, Alkaline Earths, Lanthanides, and Transition Metals” *J. Am. Ceram. Soc.* **95**, pp.1297–1303 (2012)
- [28] BREHAULT A., PATIL D., KAMATH H., YOUNGMAN R. E., THIRION L. M., MAURO J. C., CORKHILL C., MCCLOY J. S., GOEL A. “Compositional Dependence of Solubility/Retention of Molybdenum Oxides in Aluminoborosilicate-Based Model Nuclear Waste Glasses” *J Phys. Chem.*, Accepted (2018) DOI 10.1021/acs.jpcc.7b09158
- [29] TAN S., OJOVAN M. I., HYATT N. C., HAND R. J., “MoO<sub>3</sub> incorporation in magnesium aluminosilicate glasses”; *J. Nucl. Mater.* **458** (2015)
- [30] KROEKER S., SCHULLER S., WREN J. E. C., GREER B. J., MESBAH A., “<sup>133</sup>Cs and <sup>23</sup>Na MAS NMR Spectroscopy of Molybdate Crystallization in Model Nuclear Glasses”; *J. Am. Ceram. Soc.* **99** [5], pp. 1557–1564 (2016)
- [31] GREER B. J., KROEKER S., “Characterisation of Heterogeneous Molybdate and Chromate Phase Assemblages in Model Nuclear Waste Glasses by Multinuclear Magnetic Resonance Spectroscopy,” *Phys. Chem. Phys.*, **14**, pp. 7375–83 (2012)
- [32] HAND R.J., J SHORT R., MORGAN S., HYATT N.C., MOBUS G., LEE W.E “Molybdenum in glasses containing vitrified nuclear waste” Proc. VII European Society of Glass Technology Conf. Athens Greece, 25-28 April 2004. *Glass Technology* **46** (2) pp. 121-124 (2005)
- [33] ROSE P.B., WOODWARD D.I., OJOVAN M.I., HYATT N.C., LEE W.E., “Crystallisation of a simulated borosilicate high-level waste glass produced on a full-scale vitrification line”; *J. Non-Cryst. Solids.* **357**, pp. 2989-3001 (2011)
- [34] FAVRAS E.P., MITROPOULOS A.C. “What is spinodal decomposition.” paper presented at the lecture note (2008)
- [35] SCHULLER S. “From glass to crystal. Nucleation, growth and phase separation: from research to applications” book chapter “phase separation processes in glass”, *EDP Sciences*, Editor: D.R. Neuville, L. Cormier, D. Caurant, L. Montagne ISBN: 978-2-7598-1783-2 (2017)
- [36] CRUM J., MAIO V., MCCLOY J., SCOTT C., RILEY B., BENEFIEL B., VIENNA J., ARCHIBALD K., RODRIGUEZ C., RUTLEDGE V., ZHU Z., RYAN J., OLSZTA M.; “Cold crucible induction melter studies for making glass ceramic waste forms: A feasibility assessment” *Journal of Nuclear Materials*, **444**, pp 481–492 (2014).

- [37] CRUM J. V., BILLINGS A.L., LANG J.B., MARRA J.C., RODRIGUEZ C.P., RYAN J.V., VIENNA J.D., “Baseline Glass Development for Combined Fission Products Waste Streams”; AFCI-WAST-WAST-MI-DV-2009-000075. Pacific Northwest National Laboratory, Richland, WA,(2009)
- [38] VIENNA J.D., CRUM J.V., SEVIGNY G.J., SMITH G.L. “Preliminary Technology Maturation Plan for Immobilization of High-Level Waste in Glass-Ceramics” FCRD-SWF-2012-000152, REV. 0, PNNL-21714. (2012)
- [39] CRUM J.V., RODRIGUEZ C., CLOY J.MC., VIENNA J.D., CHUNG C. “Glass Ceramic Formulation Data Package” FCRD-SWF -2012-000139, PNNL-21471 (2012)
- [40] CHOUARD N., CAURANT D., MAJÉRUS O., DUSSOSSOY J.L., LEDIEU A., PEUGET S., BADDOUR-HADJEAND R., PEREIRA-RAMOS J. P. “Effect of neodymium oxide on the solubility of MoO<sub>3</sub> in an aluminoborosilicate glass.”; *J. Non-Cryst. Solids.* **357**, pp 2752-2762 (2011).
- [41] TAURINES T., BOIZOT B. “Microstructure of powellite-rich glass-ceramics: A model system for high level waste immobilization.”; *J. Am. Ceram. Soc.* **95**, pp 1105-1111 (2012)